An X-ray Study of the Galactic Shell-type Supernova Remnants Using XMM-Newton and Chandra

Nergis Cesur[1], Aytap Sezer[2], Murat Hüdaverdi[1]
[1]Yıldız Technical University, Istanbul, Turkey
[2]Avrasya University, Trabzon, Turkey

ABSTRACT

We present the results of a study of the Galactic supernova remnants (SNRs) **Cas A**, **RCW86, SN1006**, **RX J1713.7-3946** and **Vela Jr.**, which are well-known members of the shell-type SNRs. They have limb-brightened morphologies in both X-ray and radio bands. Due to the emphasised importance of background estimation in spectral analysis in plenty of studies, ***POWER-LAW*** and ***APEC*** models were used to analyze Cosmic X-ray Background (CXB), Galactic Ridge X-ray Emission (GRXE) and Local Hot Bubble (LHB) components of background emission with calculating the Galactic hydrogen column density (N_H) and electron temperature (kT_e). Using archival data from *XMM-Newton* and *Chandra*, we investigate the thermal and non-thermal X-ray emission, the ionization states and the plasma structures of these SNRs by extracting the X-ray spectra from different regions across the remnants.

INTRODUCTION

Shell-type SNRs, whose appearance is characterized by a limb-brightened shell formed by the ejecta from the SN explosion and afterwards also by the swept up surrounding material, have dense outer layers that emitting more when compared with the other regions of the SNR. But also, in young SNRs, the dense emission may be caused by the reverse shock that has not reached the inner ejecta yet. In these both cases, the limb-brightening provides the shell-like morphology. Shell-type SNRs have bright morphology both in X-ray and radio bands, but not bright emission associated with central region. Due to show the importance of background estimation, **RX J1713.7–3946** selected as a sample for the analysis, whose progenitor mass is about 12 $M_\odot$ – 16 $M_\odot$ and lies at a distance of 1.3 ± 0.4 kpc, probably in the Sagittarius galactic arm (Cassam-Chenaï et al., 2004).

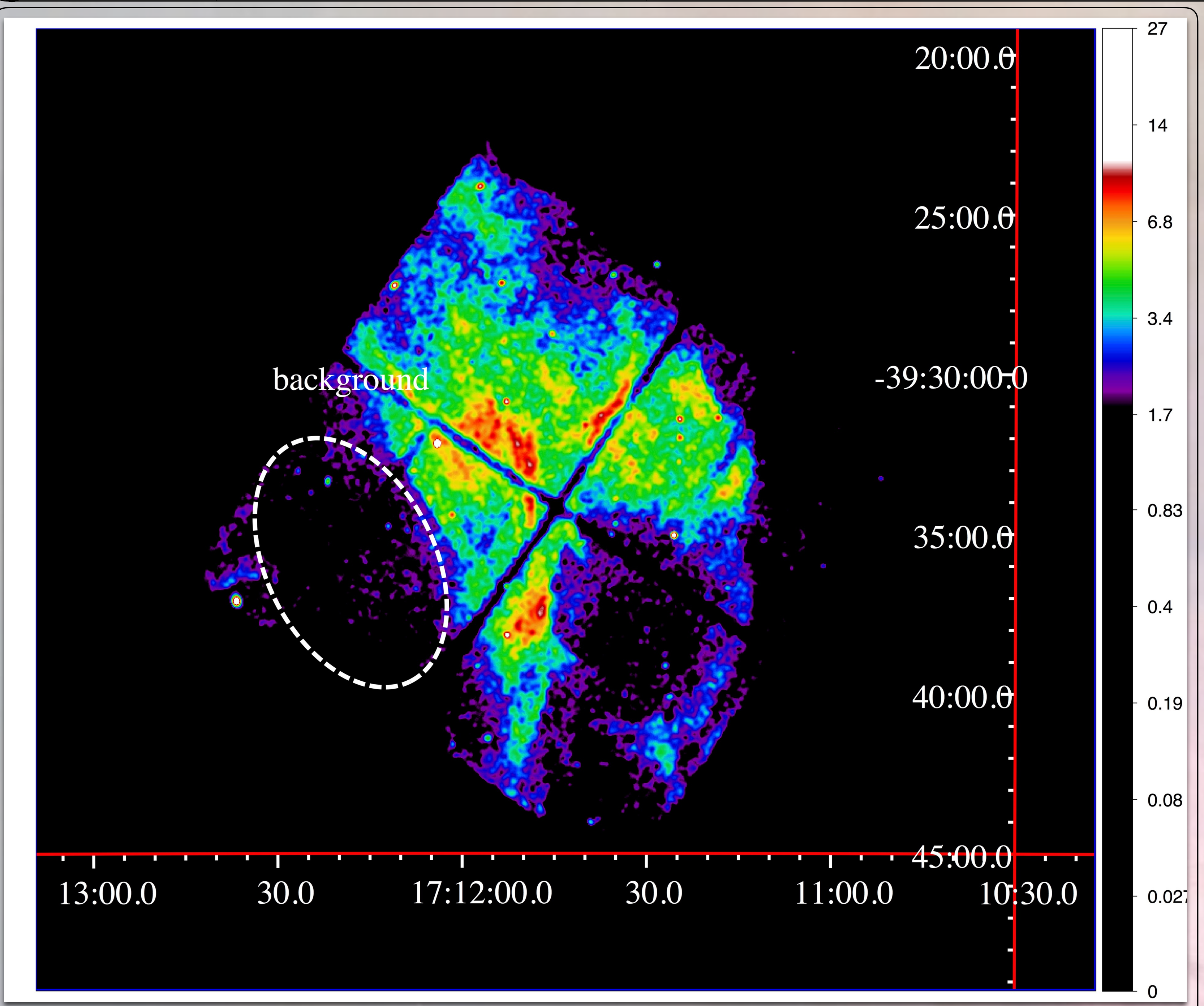

Figure 1. 0.5 – 7.0 keV X-ray image of Northwest of **RX J1713.7–3946**. The background region was selected from a source-free area in the same FoV. The color scale corresponds the image counts.

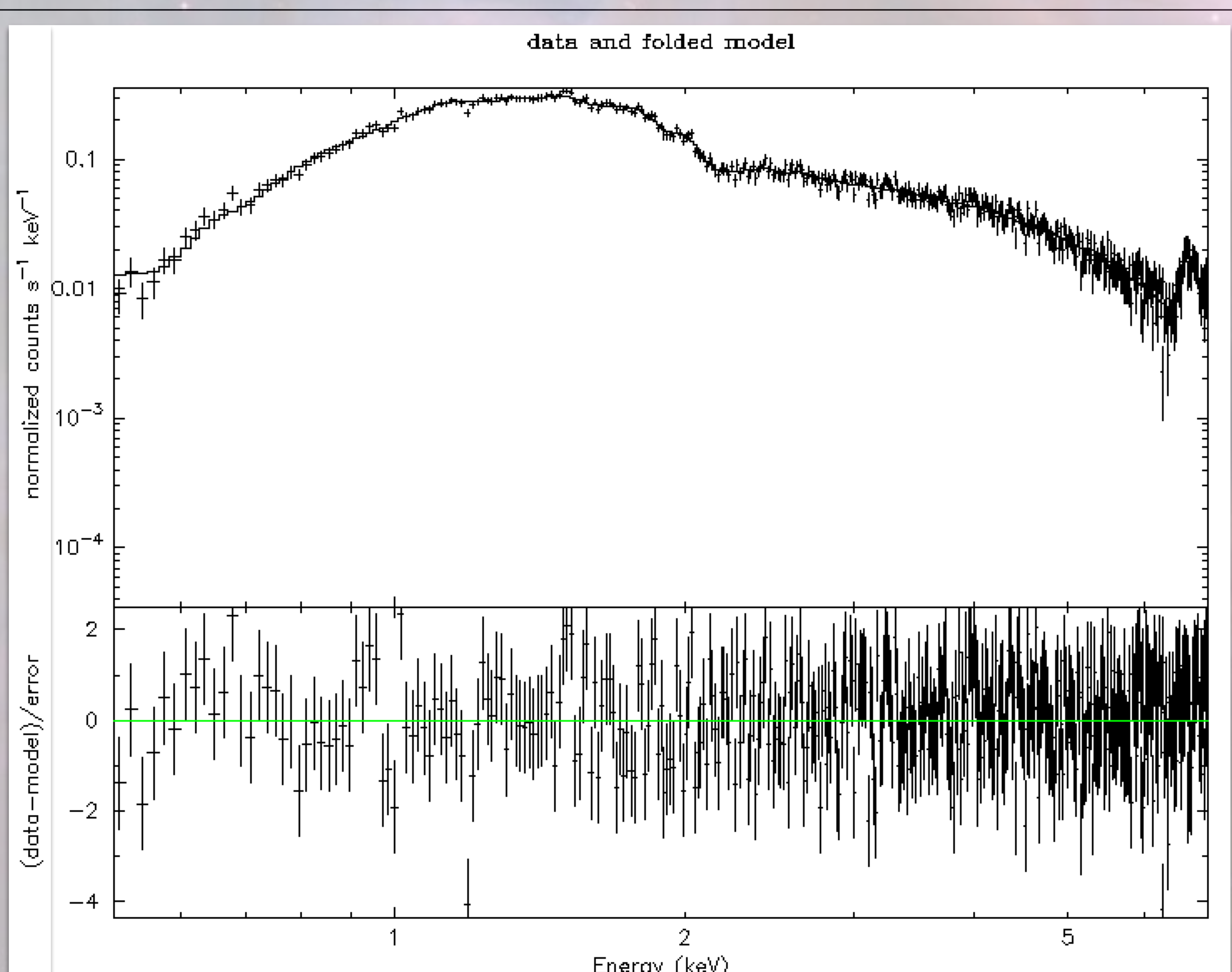

Figure 2. Chandra spectral plot of the simulated background region in the 0.5 – 7.0 keV energy band.

Table 3: Best-fit parameters for the background spectrum of Northwest of RX J1713.7–3946.

Parameters	Values
CXB	
N_H (10^{22}cm^{-2})	1.38 *(fixed) (Kalberla et al., 2005)*
Photon Index	1.41 *(fixed) (Kushino et al., 2002)*
S. B.†($ergs^{-1}$cm^{-2}arcmin^{-2})	5.41×10^{-15} *(fixed) (Kushino et al., 2002)*
GRXE	
N_H (10^{22}cm^{-2})	$2.202^{+0.205}_{-0.171}$
kT_e (keV)	$0.488^{+0.041}_{-0.031}$ *(LP)*
norm (10^{-2} photons cm^{-2} s^{-1})	$1.564^{+0.041}_{-0.003}$
kT_e (keV)	$8.920^{+1.291}_{-0.849}$ *(HP)*
norm (10^{-2} photons cm^{-2} s^{-1})	$0.410^{+0.001}_{-0.001}$
LHB	
kT_e (keV)	$2.504^{+1.537}_{-0.681}$
norm (10^{-2} photons cm^{-2} s^{-1})	$0.216^{+0.001}_{-0.001}$
χ^2/dof	424.41/436

† *S. B.: Surface Brightness in the 2–10 keV band.*

We fitted the X-ray background spectrum with the model:

$$N_{H(CXB)} \times CXB + N_{H(GRXE)} \times (HP+LP) + LHB$$

CXB parameters were fixed to those of Kushino et al., 2012. The other parameters were set free because of spatially variability.

Table 1: General information for each SNR.

SNR	Angular Size (Radio)	Position RA/DEC (J2000)	Age (year)
Cas A	5′	23:23:24 +58:48:54	316-352 *(Fesen et al.,2006)*
RCW 86	42′	14:43:00 -62:30:00	2000-10000 *(Vink et al.,2006)*
RX J1713.7-3946	65′x55′	17:13:28 -39:49:48	1000-2100 *(Tsuji & Uchiyama, 2016)*
SN1006	30′	15:02:50 -41:56:00	~ 1011 *(Dyer et al.,2001)*
Vela Jr	120′	08:52:00 -46:20:00	2400-5100 *(Allen et al.,2015)*

Table 2: XMM-Newton and Chandra log of archival observations used in the study for each SNR.

SNR	Observatory	Obs. Id.	Obs. Date	Detector	Exp. (ks)
Cas A	Chandra	4639	2004-04-25	ACIS-S	80
Cas A	XMM-Newton	0412180101	2006-06-22	MOS2&PN	59
RCW 86	Chandra	1993	2001-02-01	ACIS-S	93
RCW 86	XMM-Newton	0504810401	2007-08-23	MOS2&PN	73
RX J1713.7-3946 (SW)	Chandra	5561	2005-07-09	ACIS-I	29
RX J1713.7-3946 (NW)	Chandra	12671	2011-07-01	ACIS-I	91
SN1006 (NW)	Chandra	13737	2012-04-20	ACIS-S	88
SN1006 (S)	Chandra	13742	2012-06-15	ACIS-I	80
SN1006 (SE)	Chandra	13741	2012-04-25	ACIS-I	99
SN1006 (SW)	Chandra	13739	2012-05-04	ACIS-I	101
SN1006 (W)	Chandra	13738	2012-04-23	ACIS-I	74
SN1006 (SE)	XMM-Newton	0306660101	2005-08-21	MOS2&PN	34
SN1006 (SW)	XMM-Newton	0653860101	2010-08-28	MOS2&PN	130
Vela Jr. (NW)	Chandra	3846	2003-01-05	ACIS-S	39
Vela Jr. (N)	Chandra	9123	2008-08-31	ACIS-S	40

ANALYSIS

In our analysis, we used Heasoft 6.20, CALDB 4.7.2, CIAO 4.8, XMM-SAS 16.0.0, XSPEC 12.9.1, SAOImage DS9 7.3.2 and AtomDB 3.0.8. N_H and kT_e were calculated for the background of the **RX J1713.7–3946**. We selected a source-free background region in the same field of view (FoV) and fitted the spectrum of this region (Figure 1) with a model of *(Abs1 ×* ***POWER-LAW****) + (Abs2 × (****APEC*** *+* ***APEC****)) + (****APEC****)*, where absorbed two-temperature ***APEC*** component represents the GRXE emission which represents the *high-temperature plasma* (HP) and *low-temperature plasma* (LP), while absorbed ***POWER-LAW*** model represents the CXB emission and the third CIE plasma model represents the LHB. The ***TBABS*** model is used for the first and second hydrogen column density values (Wilms et al., 2000). While applying the model, the fixed hydrogen column density parameters of CXB component (Bamba et al., 2016) are provided by Kalberla et al. (2005) for the remnant. The results are shown in Table 3. As a final step, the background spectrum is simulated with the ***FAKEIT*** command (Figure 2).

RESULTS & DISCUSSION

GRXE component of the selected background region was found to have the values of kT_{HP} ~ 0.48 keV, kT_{LP} ~ 8.92 keV, the $N_{H(GRXE)}$ was found to be ~ 2.02 × 10^{22} cm^{-2}, and LHB component was found to have the kT_e value of ~ 2.50 keV. In the next step, we will discuss the effects of background modelling according to the values based on subtraction of estimated different backgrounds from source spectra. We will repeat the same method for our other selected SNRs, as well. While estimating the background of each remnants, we will also consider the environment where the remnants are located in, for example, the distance from the galactic plane. Thus, the contribution of the background to the morphological and spectral properties of SNRs will be discussed in such an analysis. Once the background analysis is finished, we will model the background subtracted spectra of each SNR using a combination of thermal and non-thermal models. We will apply the models such as ***VNEI***, ***VPSHOCK***, ***VAPEC*** under XSPEC for thermal emission, and ***POWER-LAW*** or ***SRCUT*** models for non-thermal emission from the SNR. We will investigate the contribution of the ejecta and interstellar medium from the each SNR. We will also study the variations in spectral properties, such as temperature and element abundances throughout the remnants.

References

Allen, G. E., Chow, K., DeLaney, T., et al., 2015, ApJ, 798, 2
Bamba, A., Terada, Y., Hewitt, J., et al., 2016, ApJ, 818,1
Cassam-Chenaï, G., Decourchelle, A., Ballet, et al., 2004, A&A, 427, 199-216
Dyer, K. K.; Reynolds, S. P.; Borkowski, K. J, 2001, ApJ, 551, 439-453, 1
Fesen, R. A., Hammell, M, C., Morse, J., et al., 2006, ApJ, 645, 283-292, 1
Kalberla et al. 2005, Astronomy & Astrophysics, 440, 775
Kushino, A., Ishisaki, Y., Morita, U., et al., 2002, PASJ, 54, 327-352, 3
Tsuji, N. & Uchiyama, Y., 2016, PASJ, 68, 6
Vink, J., Bleeker, J., van der Heyden, K., et al., 2006, ApJ, 648, L33-L37, 1
Wilms J., A. A., & McCray R., 2000, ApJ, 542, 914